

The Computational Modeling of Falling Film Thickness Flowing Over Evaporator Tubes

I. A. Hassan^{*,a}, A. Sadikin^b, and N. Mat Isa^c

Universiti Tun Hussein Onn Malaysia (UTHM), 86400 Parit Raja, Batu Pahat, Johor, Malaysia.

^{a,*}izzudinshah32@yahoo.com, ^bazmah@uthm.edu.my, ^csikin@uthm.edu.my

Abstract – *This paper presents a computational modeling of water falling film flowing over the horizontal tubes of evaporator. The objective of this study is to use numerical predictions for comparing the film thickness along circumferential direction of tube on 2-D CFD models. The results are then validated with a verification of correlation in previous literatures. A comprehensive design of 2-D models have been developed according to the real application and actual configuration of the falling film evaporator as well as previous experimental parameters. A computational modeling of the water falling film is presented with the aid of Ansys Fluent softwares. The Volume of Fluid (VOF) technique is adapted in this analysis since its capabilities of determining the film thickness on tubes surface is highly reliable. The numerical analysis is carried out under the influence of the pitch tube at temperature of 27°C and ambient pressures. Three types of CFD numerical models were used in this simulation with tubes spacing of 30 mm, 20 mm and 10 mm respectively. The use of a numerical simulation tool on water falling film has resulted in a detailed investigation of film thickness. Based on the numerical simulated results, it is found that the average values of water film thickness for each model are 0.1858 mm, 0.1904 mm, 0.2052 mm, and 0.2200 mm. Copyright © 2015 Penerbit Akademia Baru - All rights reserved.*

Keywords: Falling Film Thickness, CFD, Horizontal Tubes, VOF, Falling Film

1.0 INTRODUCTION

A falling film evaporator is an industrial device to concentrate or remove desired elements from main solutions by the method of falling film evaporation. The evaporation process take place on its heat sensitive components and under the influence of low pressures. This type of heat exchanger is particularly useful in application where temperature different between heating medium and the liquids is less than 8°C[1]. It has made a number of important applications ranging from desalination industries, refrigeration systems, chemical, food and dairy industries [1]. The design of falling film evaporator is made of 4 to 8 metres long tubes which are heated by steam or vapor. In recent years, there are also applications used primarily for desalination and refrigeration technology where the process fluid evaporates on the outside of horizontal tube bundle. The increasing use of horizontal falling film evaporator to remove undesired minerals from saline water has brought an impact to the conventional heat exchangers such as the coil and flooded evaporators. They have received less attention and being replaced gradually in recent years. In air conditioning and refrigeration applications, the falling film are

not widely due to difficulties in liquid distribution and tube alignment, which affect flow uniformity and dryout, especially in deep bundles [2].

1.1 Falling Liquids Film

In configuration of horizontal falling film evaporator, the liquid to be evaporated is sprayed on horizontal tubes as shown in figure 1.

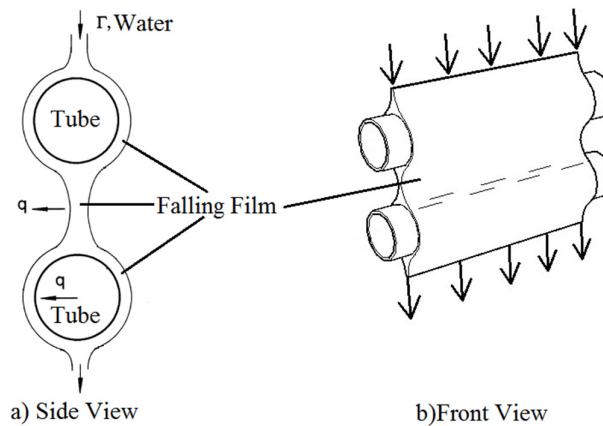


Figure 1: Schematic for the flows of falling liquids film on horizontal tubes modified from [3] and [4]

When a liquid is applied uniformly to the outside and top of a horizontal tube, it flows in a layer form around the periphery and falls off the bottom. The gravitational influence of this fluid flow is called falling liquids film[2]. A falling liquids film flows over a surface of a horizontal tube have been widely applied as a configuration of heat exchangers. Water drips from the underside of the upper tube, falls freely in the intertube space, impinges onto the next tube and flows at the tube circumference as a film. The internal properties of this flows are usually dominated by viscous, gravity and surface tension effects[3].

The modes of flow patterns on horizontal tube of falling liquids film on plays an important role in the heat and mass transfer process. The complex nature of these events have received wide attention from many researchers. Many theoretical and experimental studies has provided valuable contributions. They are generally observed by means of control over the mass flow rate and other physical parameters include pitch length, shape of tube surface, and kinds of fluids used [1]. Basically, the flow modes are classified into three different patterns when falling liquid films is flowing over horizontal cylinders. Each of these flow patterns is known as droplet mode, the jet or column mode and the continuous liquid sheet mode as shown in Fig 2.5.

1.2 The Summary on Previous Works

In general, the heat transfer through the tube wall is dependent on the thickness of tube, surfaces roughness and thermal conductivity of the material used. Stainless steel has a relatively low thermal conductivity compared with copper[4]. The significant factors influenced the film thickness on the surface of horizontal plain tube are intertube spacing, circumferential angle, and the film's Reynolds number [5]. The high heat transfer of falling liquid film on horizontal

tubes is in the form of a very thin film[5]. The work of [6] also concluded that heat transfer decrease with an increase of film flow rate. According to[7], the heat transfer magnitude is directly related to the thickness of the film and whether or not the film is laminar or turbulent. Meanwhile, parken, armbruster and mitrovic, it seems that temperature effect of horizontal falling film is closely related to the decrease of viscosity and consequent decrease in the film thickness [6].

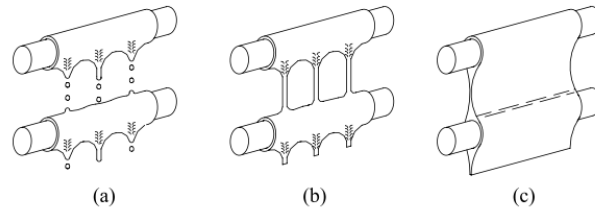


Figure 2: Schematic of the three main inter-tube flow modes a) droplet mode, b) column or jet mode and c) sheet mode [3]

Many previous experiments on falling film thickness have been reviewed by [2] and [7]. Their results concluded that the increase in the film thickness will reduce the heat transfer rates. The work of D. Gstohl and JR Thome is one among the review of [7] which has been agreed with the conclusion. The measurement of falling film thickness on horizontal tubes is carried out by micromasuring instrument [8], [9]. According to [2], the increases of convective heat transfer temperature h with liquid temperature effect are closely related to the decrease of viscosity and consequent decrease in the film thickness. Based on the result of [10] in figure 3, they concluded that film thickness around horizontal tube increases with the flow rate of water film and it is directly proportional to Reynolds number.

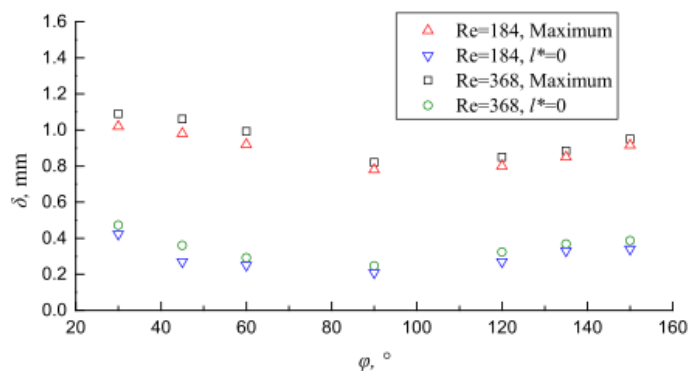


Figure 3: The film thickness around horizontal tube increases with the Reynolds number of water film [10].

His conclusions has justified the experimental results of [11] in figure 4 below which concluded that the effect of increasing the water film flow rate leads to heat transfer increased.

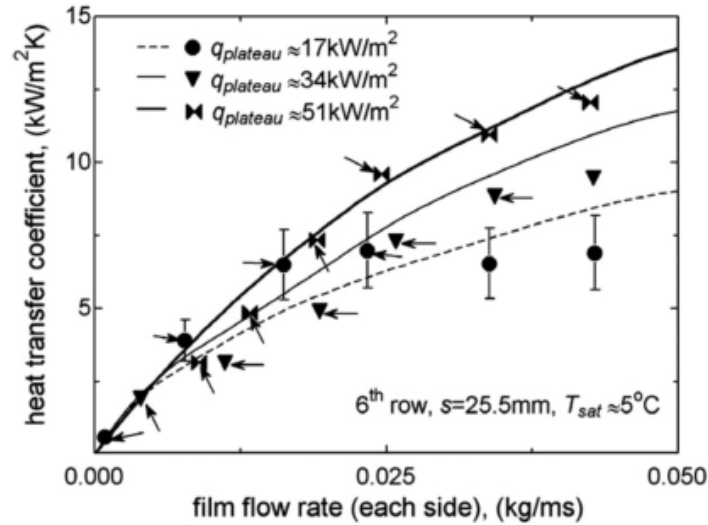


Figure 4: The effects of film flow rate on the heat transfer coefficient according to the experimental results of [11].

In addition, the review of [5] shows that experimental results of [8] have proposed a new correlation for measuring the film thickness. It is provided the expected value of the plain tube film thickness in the range 0 - 180 °.

$$\delta = c \left(\frac{3\mu_L \Gamma}{\rho_L (\rho_L - \rho_G) g \sin \beta} \right)^{1/3} \left(\frac{H}{d} \right)^n \quad (1)$$

where H is inter tube spacing or feeder height, d is diameter, β is orientation angles along tube circumferential direction, c is constant, ρ_G is mass density of air, and ρ_L is mass density of water. Another correlation of falling film thickness has been reviewed by [4] as shown below. The correlation is based on work of Rogers and Goindi and it gives a minimum film thickness at orientation angle of 90 degrees only.

$$\left(\frac{\delta}{d} \right)_{\min} = 1.186 (Re_L)^{\frac{1}{3}} Ar^{-\frac{1}{3}} \quad (2)$$

where Re_L is Reynolds Number of falling liquid film, δ is falling film thickness on tube surface, d is external diameter of tube, and Ar is Archimedes Number. According to [4], the values of Archimedes Number is 10^{10} . The trends line of correlation 1 in graph is based on figure 2.14. Although, the decreases of the film thickness with the increase of circumferential angles occur until reaching a minimum values near 90°, it is then increases until reaches 170°.

According to the studies of [8] and [10], the film thickness decreases as the tube spacing increases as shown in figure 6 and figure 7 below. In figure 3, [8] has used the classical Nusselt correlation equation intensively as a basis for comparison with the experimental data. Both graphs are almost identical except for the result of [8] is extended to a wide range of Reynolds number. The result in figure 7 shows that film thickness is slightly increased while the tube spacing ranging from 20 to 40 mm. Due to the effect of gravity, the larger tube spacing means longer distance for being accelerated. Hence, the velocity of the liquid film increases with the tube spacing at the same spray density, which makes the film thinner [10].

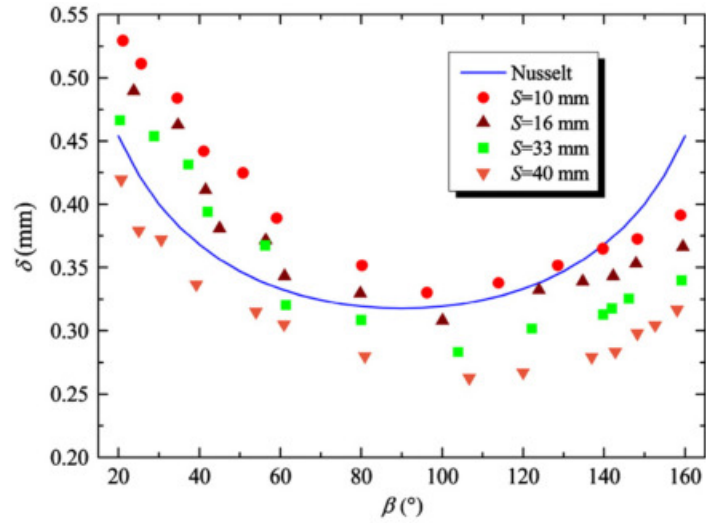


Figure 5: Variation in film thickness with circumferential angles [8].

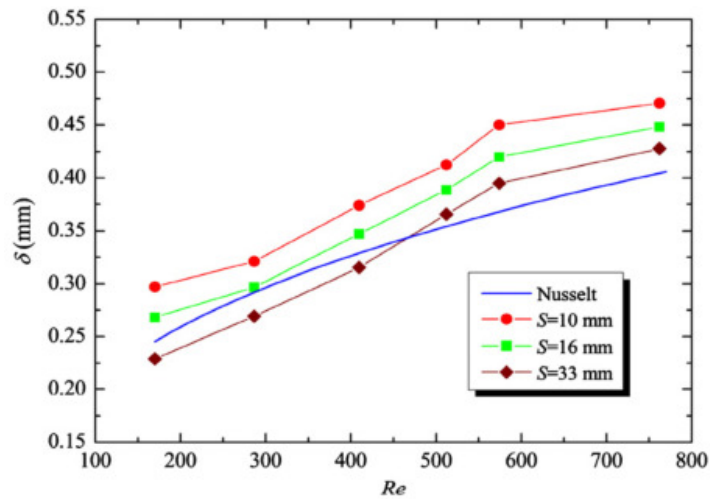


Figure 6: Variation of film thickness at different intertube spacing [8]

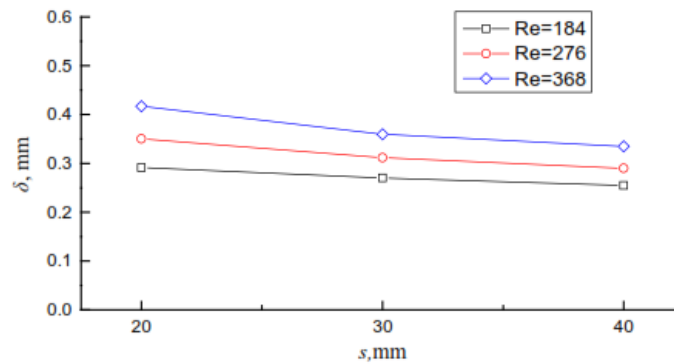


Figure 7: The effect of tube spacing on film thickness [10].

Based on the review of [2], various length of tube spacing were used according to the requirements need in their studies. However, these values are within the specified range starting from a minimum value of 2 mm up to a maximum value of 100mm. According to previous studies provided by [2], the tube spacing were commonly used in experiments are in the range between 2mm to 51mm.

The purpose of present work is to investigate the influence of pitch tube on falling film thickness at fixed mass flow rates. The research is almost the same as the experimental methods of (X. Chen et al. 2015) and (Hou et al. 2012) but it was conducted by means of numerical simulation. In the numerical analysis, the configurations of horizontal plain unheated tubes and all proposed parameters are adopted by referring to the results of previous literatures. In all cases, the water is selected as working fluids while the air is assumed to be filled in empty space of 2D CFD models. The film Reynolds number is fixed at 800 in order to comply with the requirements of equation 2. Meanwhile, the horizontal tubes with diameter of 20mm (\approx 0.75 inch) are selected with 3 pitch tube sizes of 10mm, 20mm and 30mm. Besides, the assigned material for tube of 2D CFD models is stainless steel.

2.0 METHODOLOGY

2.1 Physical model

The physical geometry of 2D numerical model is constructed using Ansys Fluent simulation software with a local body of influence techniques in meshes. The single in-line arrangement of two tubes formed a configuration as shown in Fig. 8.

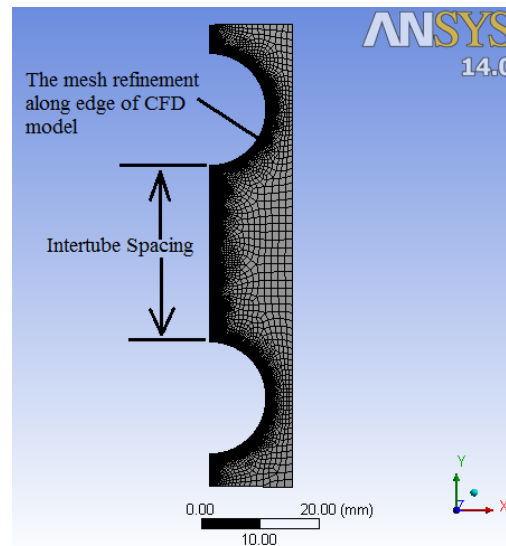


Figure 8: The 2D half symmetrical mesh model with edge sizing of 0.1mm

Both tubes have diameter of 19.05 mm with 3 different sizes of tube spacing. These are 10mm, 20mm, and 30mm. The tube cylinder wall are considered as a smooth surfaces.

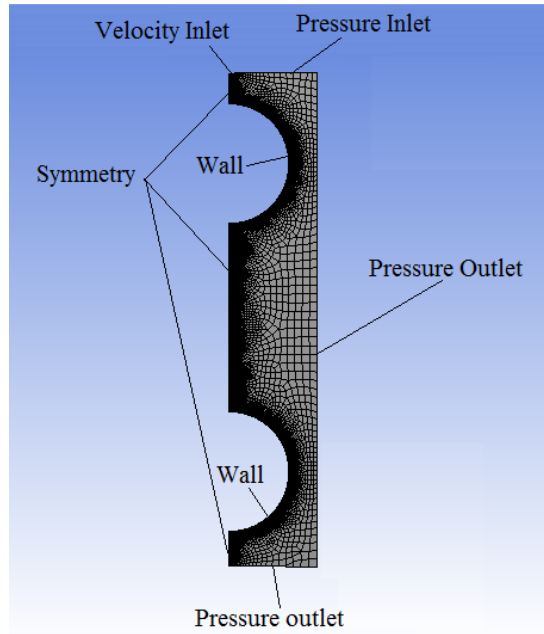


Figure 8: Boundary conditions for 2D CFD model

The boundary for water flow inlet is on top surface of the CFD numerical model. It was set as a velocity inlet, where the water liquid flows downward uniformly at different velocities. The remaining top and back boundaries are set as the pressure inlet while the bottom boundary is the pressure outlet. The front and both sides of this model are considered as the symmetrical boundary conditions.

The symmetrical and tube wall edges have been meshed using a edge sizing techniques. All mesh refinement size is 0.1 mm and applied with fluent default setting. This refinement technique making it possible to observe the thickness of falling liquid film in detail near the test tube surface. The falling water film flows over the upper tube is under combined effect of the gravity to the bottom of test tube. The flow is also directly influenced by adhesive and viscosity characteristics of water to the walls of the tubes.

2.2 Properties of fluids

In this simulation analysis, water is used as the working fluids. The flow behaviour of working fluids mostly depend on Reynolds Number of liquid film and it is defined according to

$$Re_L = \frac{4\Gamma}{\mu} \quad (3)$$

where Re_L = film Reynolds number, Γ = film flow rate per unit of tube length and μ = Newtonian dynamic viscosity of liquid film. The velocity inlet V_L is a parameter adopted in numerical modelling of Fluent software. It is closely related with several variables including dynamic viscosity, hydraulic diameter, Reynolds Number and liquid mass density of falling liquid film. According to definition of [8], the Reynolds number in term of velocity inlet is defined as

$$V_L = \frac{\mu Re}{\rho D_h} \quad (4)$$

where μ is newtonian dynamic viscosity of liquid film, D_h is hydraulic diameter of water inlet, Re is Reynolds Number and ρ is liquid mass density. Many previous researchers have tried to determine an accurate values of Reynolds number whether treated as being laminar nor turbulent. The experiments of Ouldhadda et al. reviewed by [12] showed that falling liquid film is considered to be laminar when the film Reynolds number is between 400 and 4 000. Based on the experimental work of [13], the film Reynolds number Re for laminar was from 150 to 800 and typically cited to be 1600–1800 for transition to turbulent flow. The Reynolds number of falling film flowing over horizontal tubes is rarely exceeds 2100[9]. In addition, the review of [10] shows that experimental results of G. Kocamustafaogullari has given a certain ranges of Reynolds number as shown in the table 1.

Table 1: Reynolds number ranges for falling liquid film [10]

Scenarios	Re
Flow pattern (a) – (b)	150 - 200
Flow pattern (b) – (c)	315 - 600
Flow regime laminar - turbelant	1000 - 2000
Typical MED Conditions	500 - 2000

The flow range of falling films applied in this simulation was treated as being laminar since its $Re = 1000$. The turbelant flow settings will take over the sheet flow mode. All properties of fluids are listed, as shown in Table 2.

Table 2: Properties of test fluids

Properties	Values
Water density (kg/m^3)	996.6
Water viscocity (kg/ms)	0.0008538
Air density (kg/m^3)	1.176
Air viscocity (kg/m-s)	0.18582e-5
Temperature	(27°C) 300.15K
Pressure	1 atm (101.42kPa)

The Volume of Fluid (VOF) model was selected for simulation with assumption that some of water evaporation is neglected. It is useful tool for tracking free surface flow on tubes. The volume fraction figures shows the film distribution on the wall of tubes and flow patterns between tube spacing. These characteristics will vary with flow rate. The explicit scheme allows analysis to use variable time stepping in order to automatically change the time-step when an interface is moving through dense cells or if the interface velocity is high. The model is analyzed at velocity inlet $V_L \geq 0.5139\text{m/s}$. Table 3 summarizes all simulation settings of Ansys Fluent software for this CFD model.

The corresponding mass flow rate to its velocity inlet is then recorded when a proper film distribution is achieved in simulation result. The thickness of water sheet film on tube surface is then measured based on angles of 15°, 30°, 45°, 60°, 75°, 90°, 105°, 120°, 135°, 150°, and 165° as shown in figure 8. These angles have been set as a reference values in accordance with many previous references such as [4]. The numerical results have been analyzed in CFD-Post where 4 mm length of measurement lines were positioned normal to tube surface. These measurement lines acted as a parameters that measures water film thickness at specified angles as shown in Fig. 9.

Table 3: Fluent simulation settings

Setting	Option
Solver	Transient
Model	VOF
Material	Water liquid
Viscous model	Laminar for $V_L = 0.52$ m/s
Pressure-velocity coupling	PISO for incompressible
Pressure	Body force weighted
Momentum	2nd order upwind
Energy	1st order upwind
Volume fraction	Geo-reconstruct
Surface tension force	CSS model (continuum surface stress)
Time steps	Variable

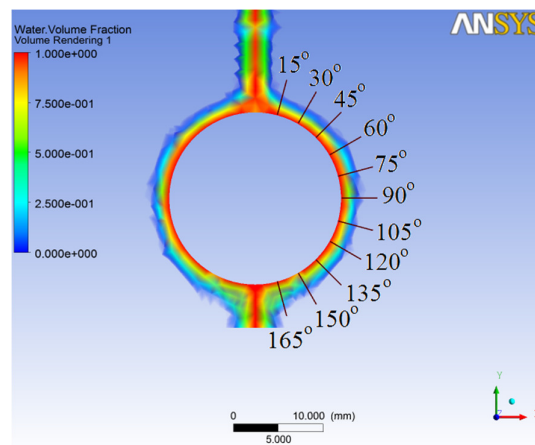


Figure 8: The orientation angles of film thickness measurements on tube surface

The thickness of water film are extracted and plotted in a graph of thickness versus orientation angles. Each measurement data is measured by taking into account the difference of water volume fraction length which only 1.

3.0 RESULTS AND DISCUSSION

In the following, we first present typical simulation results of water film thickness for sheet flow modes. These visual result are shown in figure 9, 10 and 11. The results of numerical analysis is ended when each flow on model has been completely transformed into sheet flow mode. In addition, all results must converged before analysis ended.

The CFD model in figure 9 with intertube spacing of 10mm is fully wetted at time of 1.06114s. This contour indicates a condition of water represented by water volume fraction between 100%. In addition, there are a two spots on separation phenomena under tube this condition existed at the bottom of the tube due to separated flow. The comparison of film thickness on CFD models have been compared in table 4 using equation and plotted in figure 10. The percentage of change between both results are quite different especially on orientation angles of 90°, 105°, and 120°.

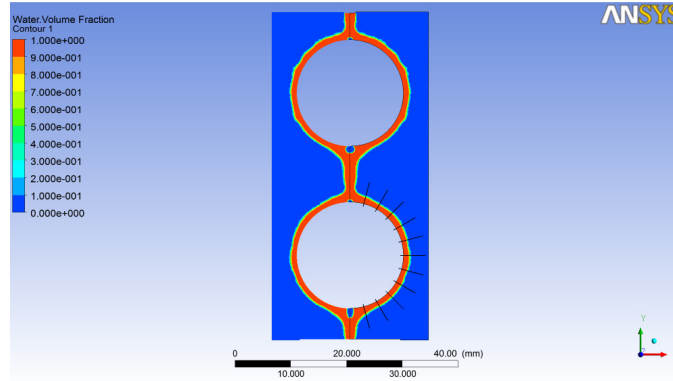


Figure 9: The 10mm CFD model is fully wetted at 1.06114s

Table 4: The Thickness Comparison for 10mm CFD Model of Intertube Spacing

Orientation Angles	The Thickness of Falling Liquids Film on Different Pitch tubes (mm)		
	10mm Intertube Spacing		% Change
	Numerical Results	Equation Results	
15	0.9184	0.6672	37.64%
30	0.6429	0.5357	20.00%
45	0.8265	0.4772	73.21%
60	0.8265	0.4460	85.32%
75	0.8265	0.4301	92.17%
90	0.9184	0.4252	115.98%
105	0.8265	0.3743	120.82%
120	0.8265	0.3881	112.96%
135	0.7347	0.4153	76.91%
150	0.6429	0.4661	37.92%
165	1.0102	0.5805	74.02%
Average	0.8182	0.4732	72.89%

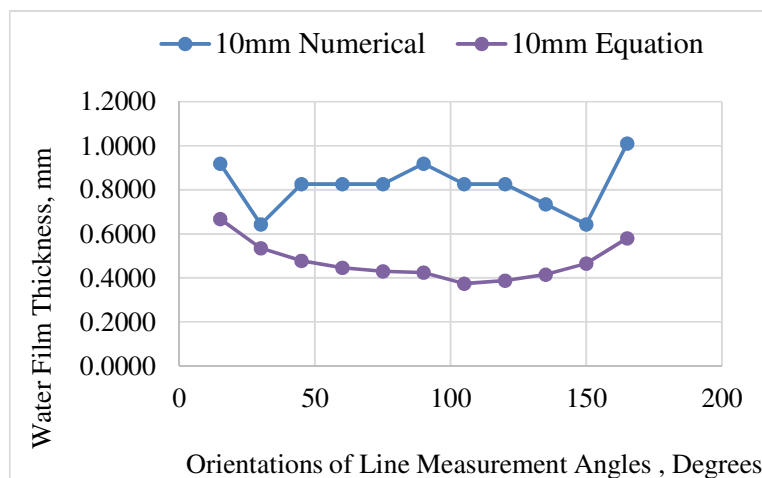


Figure 10: Graph of water film thickness for 10mm CFD Model of Intertube Spacing

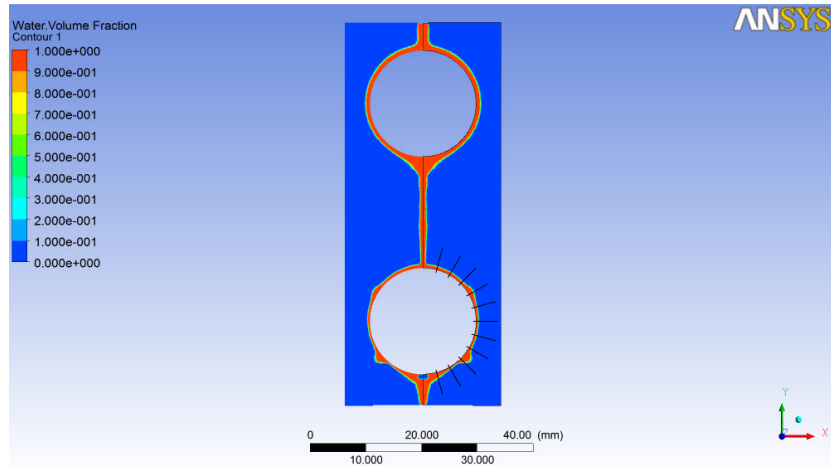


Figure 11: The 20mm CFD model is fully wetted at 0.220653s

Table 5: The Thickness Comparison for 20mm Intertube Spacing

Orientation Angles	The Thickness of Falling Liquids Film on Different Pitch tubes (mm)		
	20mm Intertube Spacing		% Change
	Numerical Results	Equation Results	
15	0.5510	0.5815	-5.24%
30	0.5510	0.4772	15.47%
45	0.5510	0.4252	29.59%
60	0.4592	0.3974	15.54%
75	0.4592	0.3832	19.83%
90	0.3673	0.3788	-3.02%
105	0.3673	0.3338	10.05%
120	0.3673	0.3462	6.11%
135	0.3674	0.3704	-0.82%
150	0.3673	0.4157	-11.63%
165	0.9184	0.5178	77.36%
Average	0.4842	0.4207	15.11%

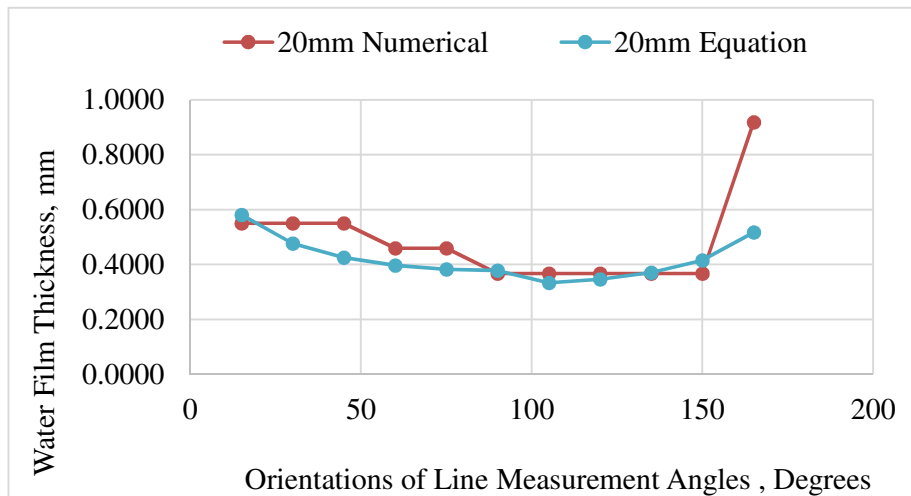


Figure 12: Graph of water film thickness for 20mm CFD Model of Intertube Spacing

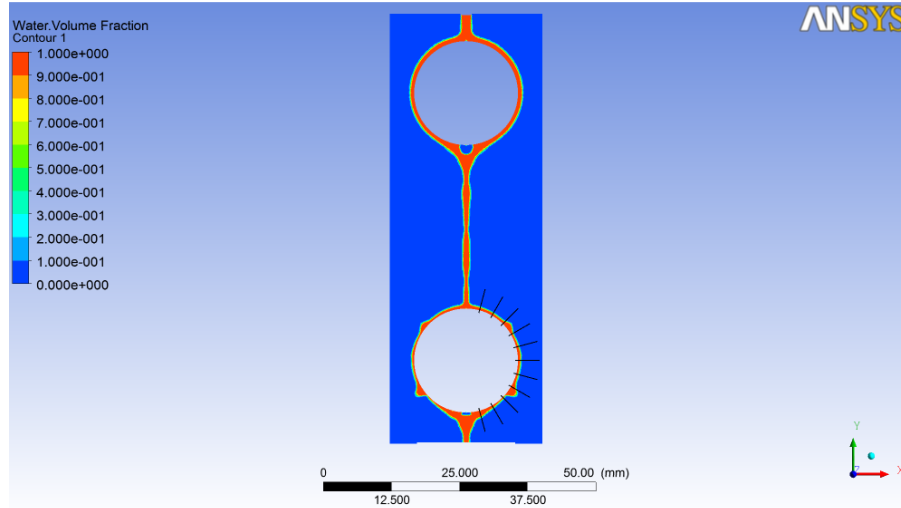


Figure 13: The 30mm CFD model is fully wetted at 0.19481s

The CFD model in Fig. 11 with intertube spacing of 20mm is fully wetted at time of 0.220653s. There are also two spots on separation phenomena under tube this condition existed at the bottom of the tube due to separated flow. The comparison of film thickness on this CFD models have been compared in table 5 using equation and plotted in figure 12. The percentage of change between numerical result and equation 1 are slightly similar with $\pm 20\%$ in error.

The CFD model in figure 13 with intertube spacing of 30mm is fully wetted at time of 0.19481s. The extracted data of film thickness have been compared in table 6 using equation and plotted in figure 14. The percentage of change between both results are slightly similar with $\pm 20\%$ in error.

Table 6: The Thickness Comparison for 30mm Intertube Spacing

Orientation Angles	The Thickness of Falling Liquids Film on Different Pitch tubes (mm)		
	30mm Intertube Spacing		% Error
	Numerical Results	Equation Results	
15	0.1837	0.5555	-66.94%
30	0.3673	0.4460	-17.64%
45	0.3674	0.3974	-7.56%
60	0.3673	0.3714	-1.09%
75	0.3673	0.3581	2.58%
90	0.2755	0.3540	-22.17%
105	0.1837	0.3123	-41.19%
120	0.2755	0.3239	-14.94%
135	0.2755	0.3465	-20.49%
150	0.3673	0.3889	-5.54%
165	0.9184	0.4844	89.59%
Average	0.3590	0.3944	-8.98%

The three comparative graphs in previous figures showed some degree of percentage errors. The angle of 0 degree is the point where water falling film collide with test tube. Water molecules will be displaced out of the point with high velocities. As a result, some disturbance waves contour existed along this point influenced the film thickness. The measurement of water

film thickness on tube surface at any orientation angles can be measured without disturbance of wave by providing several samples in slightly different time as shown in figure 15.

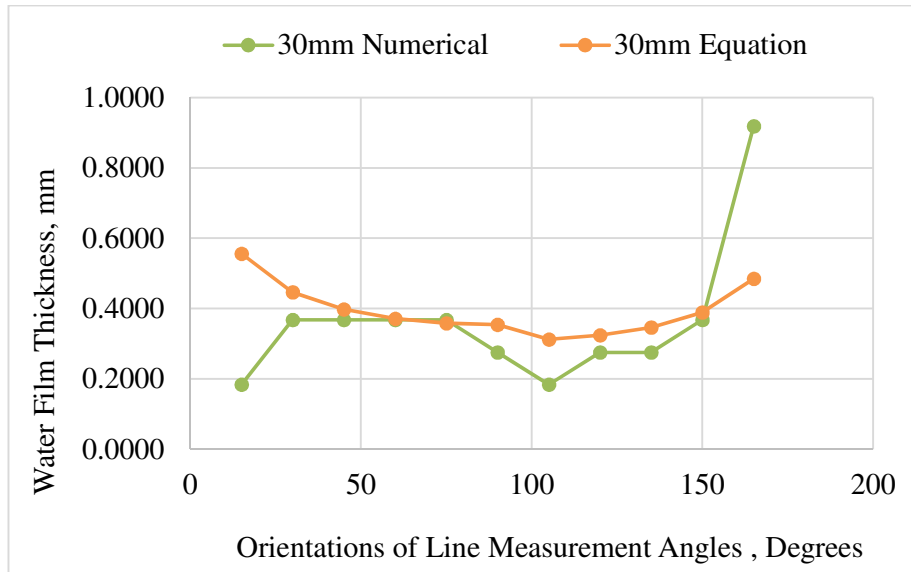


Figure 14: Graph of water film thickness for 30mm CFD Model of Intertube Spacing

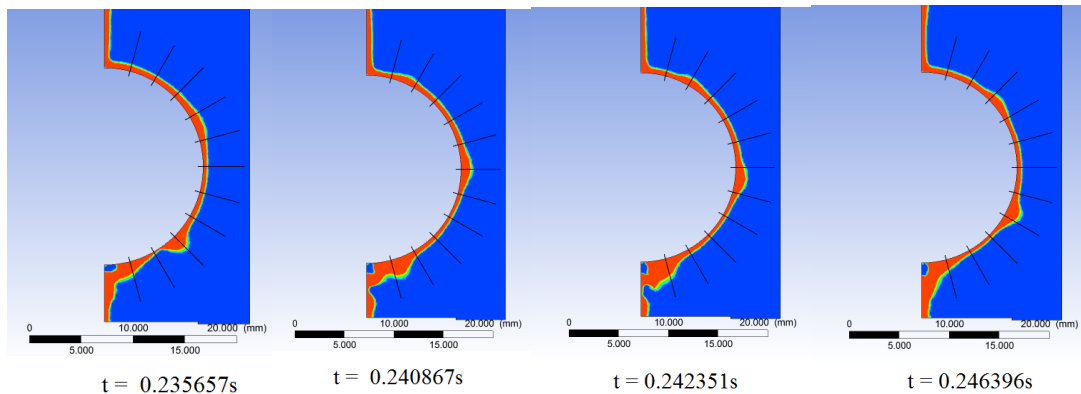


Figure 15: The disturbance of water film wave on tube surface influenced the thickness

4.0 CONCLUSION

Based on the simulation results, the thickness of sheet mode varies with orientation angles. This characteristics are affected by pitch tube. The different setting of parameters in Fluent software such time steps also lead to slightly different results. The thickness has been reduced when approaching the orientation angle of 90°. It is then increased gradually as it passed through this angle. Water molecules with inherent properties are becoming increasingly accumulating under the tube. The existing literatures has been reviewed extensively. The current numerical results are so far in agreement with the results from the literatures. The tube spacing of 30mm is a CFD model produced the thinnest film. The numerical tool chosen for

the present study, Fluent, has enabled close examination of the flow field. Further work is in progress with the addition of experimental data and extensions.

REFERENCES

- [1] M.I. Mohamed, Flow behavior of liquid falling film on a horizontal rotating tube, *Exp. Therm. Fluid Sci.* 31 (2007) 325–332.
- [2] G. Ribatski, A.M. Jacobi, Falling-film evaporation on horizontal tubes — a critical review *Evaporation d ’ un film tombant sur des tubes horizontaux — passage en revue critique* 28 (2005) 635–653.
- [3] R. Armbruster, J. Mitrovic, Evaporative cooling of a falling water film on horizontal tubes 18 (1998).
- [4] F. Jafar, G. Thorpe, O.F. Turan, Liquid Film Falling on Horizontal Circular Cylinders, no. December (2007) 1193–1200.
- [5] A.M. Abed, M.A. Alghoul, M.H. Yazdi, A.N. Al-Shamani, K. Sopian, The role of enhancement techniques on heat and mass transfer characteristics of shell and tube spray evaporator: a detailed review *Appl. Therm. Eng.*, Oct. 2014.
- [6] L. Yang, S. Shen, Experimental study of falling film evaporation heat transfer outside horizontal tubes, *Desalination* 220 (2008) 654–660.
- [7] B. Ruan, A.M. Jacobi, L. Li, Effects of a countercurrent gas flow on falling-film mode transitions between horizontal tubes, *Exp. Therm. Fluid Sci.* 33 (2009) 1216–1225.
- [8] H. Hou, Q. Bi, H. Ma, G. Wu, Distribution characteristics of falling film thickness around a horizontal tube, *Desalination* 285 (2012) 393–398.
- [9] L. Xu, M. Ge, S. Wang, Y. Wang, Heat-transfer film coefficients of falling film horizontal tube evaporators, *Desalination* 166 (2004) 223–230.
- [10] X. Chen, S. Shen, Y. Wang, J. Chen, J. Zhang, Measurement on falling film thickness distribution around horizontal tube with laser-induced fluorescence technology, *Int. J. Heat Mass Transf.* 89 (2015) 707–713.
- [11] G. Ribatski, J. R. Thome, Experimental study on the onset of local dryout in an evaporating falling film on horizontal plain tubes, *Exp. Therm. Fluid Sci.* 31 (2007) 483–493.
- [12] L. Luo, G. Zhang, J. Pan, M. Tian, Flow and heat transfer characteristics of falling water film on horizontal circular and non-circular cylinders, *J. Hydrodyn. Ser. B* 25 (2013) 404–414.
- [13] H. Hou, Q. Bi, X. Zhang, Numerical simulation and performance analysis of horizontal-tube falling-film evaporators in seawater desalination, *Int. Commun. Heat Mass Transf.*, 39 (2012) 46–51.